J. Fluid Mech. (1985), *vol.* 156, *pp.* 505–531
Printed in Great Britain

Spectral and statistical properties of the equilibrium range in wind-generated gravity waves

By O. M. PHILLIPS

Department of Earth and Planetary Sciences, The Johns Hopkins University, Baltimore, Maryland 21218

(Received 19 October 1984)

Recent measurements of wave spectra and observations by remote sensing of the sea surface indicate that the author's (1958) conception of an upper-limit asymptote to the spectrum, independent of wind stress, is no longer tenable. The nature of the equilibrium range is reexamined, using the dynamical insights into wave–wave interactions, energy input from the wind and wave-breaking that have been developed since 1960. With the assumption that all three of these processes are important in the equilibrium range, the wavenumber spectrum is found to be of the form $(\cos\theta)^p u_* g^{-\frac{1}{2}} k^{-\frac{7}{2}}$, where $p \sim \frac{1}{2}$ and the frequency spectrum is proportional to $u_* g\sigma^{-4}$. These forms have been found by Kitaigorodskii (1983) on a quite different dynamical basis; the latter is consistent with the form found empirically by Toba (1973) and later workers. Various derived spectra, such as those of the sea-surface slope and of an instantaneous line traverse of the surface, are also given, as well as directional frequency spectra and frequency spectra of slope.

The theory also provides expressions for the spectral rates of action, energy and momentum loss from the equilibrium range by wave-breaking and for the spectrally integrated rates across the whole range. These indicate that, as a wave field develops with increasing fetch or duration, the momentum flux to the underlying water by wave-breaking increases asymptotically to a large fraction of the total wind stress and that the energy flux to turbulence in the water, occurring over a wide range of scales, increases logarithmically as the extent of the equilibrium range increases. Interrelationships are pointed out among different sets of measurements such as the various spectral levels, the directional distributions, the total mean-square slope and the ratio of downwind to crosswind mean-square slopes.

Finally, some statistical characteristics of the breaking events are deduced, including the expected length of breaking fronts (per unit surface area) with speeds of advance between c and $c+\mathrm{d}c$ and the number of such breaking events passing a given point per unit time. These then lead to simple expressions for the density of whitecapping, those breaking events that produce bubbles and trails of foam, the total number of whitecaps passing a given point per unit time and, more tenuously, the whitecap coverage.

1. Introduction

The breaking of waves is a process that is ubiquitous over two-thirds of the surface of the globe. It is clearly responsible for part of the transfer of mechanical energy from the atmosphere, through waves, to turbulence near the ocean surface and of momentum to ocean currents. It leads to enhancement of the heat transfer and especially of the gas exchange between the atmosphere and the ocean as the diffusive

surface film is disrupted by breaking events and gases are diffused downwards by intense small-scale turbulence (Kitaigorodskii 1984). Breaking events also augment substantially but locally the drag of the air on the water itself, as Banner & Melville (1976) have shown.

During the past few years, a great deal of attention has been paid to the dynamics of breaking and the search for criteria under which waves might be expected to break. The remarkable theoretical developments and pioneering numerical experiments of Longuet-Higgins & Cokelet (1978) have traced the evolution of finite-amplitude gravity waves on deep water to the point of wave-breaking and just beyond, in cases where the breaking results both from the intrinsic instability of the wave and from local impulsive forcing. A notable property of these calculations is the demonstration that, in an already unstable wave, breaking occurs at wave amplitudes far less than those associated with Stokes' limiting configuration for a steady wavetrain. At very small scales, among the short gravity waves and gravity–capillary waves, the surface drift induced by the wind shear in the top couple of millimetres can also induce microscale breaking at small wave amplitudes (Phillips & Banner 1974). In spite of this, attempts have continued to find a threshold variable such as the local vertical acceleration, or possibly a combination of variables, that would determine the probability of breaking of an individual wave crest. The numerical experiments of Longuet-Higgins & Cokelet for pure gravity waves do make it difficult to associate any single local variable with the onset of breaking – it seems that the recent time history of the surface configuration is much more pertinent to the matter than a single local threshold variable.

In any event, the idea that, if the local surface acceleration at a wave crest reaches some fraction of the gravitational acceleration g, the wave would then break, lay behind the author's proposal in 1958 of an equilibrium range at high wavenumbers (and frequencies) of the wave spectrum. It was argued that, although the frequency or density of wave-breaking depends on the wind stress, the limiting configurations of the waves at any instant should not; since the spectrum is a representation of the configuration, it was postulated that the breaking process imposes an upper limit to the spectral density of wave components over wavenumbers substantially greater than that of the spectral peak, this upper limit being independent of the wind speed. The idea was, in fact, one of saturation rather than equilibrium, any excursion of the spectral density above this limit being relieved immediately by breaking. It then leads, on purely dimensional grounds, to upper-limit spectral asymptotes in the gravity-wave range of

$$\Psi(\boldsymbol{k}) \propto f(\theta)\, k^{-4}, \tag{1.1}$$

for the wavenumber spectrum and

$$\Phi(\sigma) \propto g^2 \sigma^{-5}, \tag{1.2}$$

for the frequency spectrum, where θ is the angle between the wind and the wavenumber $\boldsymbol{k}$. In the intervening 25 years or so, these expressions have been found to be useful and reasonably accurate representations for the spectral forms over frequencies and wavenumbers greater than about twice that of the spectral peaks – in fact some empirical formulas such as the JONSWAP spectrum have been forced to assume this shape at large σ.

Nevertheless, as more accurate and extensive measurements have become available, it has become increasingly more evident that the idea of a hard, saturated upper limit to the spectrum is no longer tenable. One of the first indications was the fact that the constant of proportionality implied in (1.2), rather than being an absolute constant,

appeared to be a function of fetch, as documented extensively in the JONSWAP report (Hasselmann *et al.* 1973). Values measured in the laboratory or at short fetches in the field were found to be a factor of five or so larger than those measured in the open ocean. It strains one's credulity to believe that the fetch should *directly* influence the structure of the high-wavenumber components of the wave field, since their interaction and generation lengthscales are very much shorter than even a moderate fetch. One obvious possibility was that the presence of very much longer waves or swell, their orbital velocities convecting the shorter waves, may lead to an apparent decrease in the spectral density (particularly in the frequency spectrum, where Doppler effects are strongest), but unpublished calculations by the author based on his 1981 study of long-wave/short-wave interactions gave an augmentation rather than a decrease. In evaluating the apparent variation of the constant of proportionality with fetch, it must be remembered that, in the individual sets of experiments at short fetches and in the open sea, spectral densities were measured over frequency intervals that were not very wide (typically about half a decade, with a range of spectral densities of over 100 to 1 over the range), and were frequently non-overlapping. At a given wind speed or friction velocity u_*, the range of values of u_*/c (where c is the phase speed of the components measured) may range from more than 1 to 0.5 in the laboratory or at short fetch, and from 0.3 to 0.04 in oceanic measurements; this suggests that the 'constant' of proportionality obtained by fitting (1.2) to measurements over restricted ranges may in fact be a function of the ratio of the friction velocity of the wind to the representative phase speed of the wave components in the range of frequencies measured.

Another persuasive indication that the spectral densities of short gravity waves generated by wind are not limited by a hard saturation upper limit is provided by remote sensing of the sea surface by means of the Bragg backscattering of radar signals from these components. Typical are the synthetic-aperture radar images, examples of which are to be found in Beal, DeLeonibus & Katz (1981). One notable image of the Nantucket Shoals region shows areas of enhanced return (hence enhanced spectral density of the surface-wave components) in regions of flow convergence produced by tidal streaming over relatively shallow bottom topography. It has long been recognized that the dominant waves are choppier in many regions exhibiting flow convergence (such as river estuaries with the outflow velocity decreasing seaward), but the imagery shows that this increase above the equilibrium level that is established by the wind on a uniform or zero current, extends to the shorter components as well. The relaxation rate of the wind-wave spectrum, when disturbed from equilibrium, is not infinite as it would be with a hard saturation limit, but finite.

In summary, then, it appears that, although (1.1) and (1.2) may have been found useful as a first approximation to the high-wavenumber and frequency components of the spectrum, the underlying assumption contained in them is no longer defensible. Nor, in fact, do they even provide the most accurate representation of recent, more careful and better instrumented measurements. Toba (1973) found empirically and with the aid of dimensional analysis that his wind-tunnel data was better represented by a spectrum of the form

$$\Phi(\sigma) \propto u_* g \sigma^{-4}, \tag{1.3}$$

or u_*/c times (1.2), and this has been confirmed in field observations by Kawai, Okuda & Toba (1977), Donelan, Hamilton & Hui (1977) and others. With hindsight, one can see a trend towards (1.3) in the collection of spectra shown by the author (1977) to support the form (1.2); although the envelope of spectral segments over the

considerable range does decrease as σ^{-5}, the individual spectra seem to slope rather less steeply. The matter clearly demands reconsideration – 25 years is a pretty good lifetime for the simple ideas underlying (1.1) and (1.2), and if they are found to be no longer viable, they should be saluted and interred with dignity.

In the present paper, we intend to take advantage of the insights developed since 1960 concerning wave interactions, energy transfer from wind to waves and the energy-loss characteristics of breaking waves, in order to place on a firmer dynamical basis our description of this part of the wind-wave spectrum. In doing so, we are led not only to a frequency spectrum of Toba's form (1.3) and to its counterpart wavenumber spectrum, but also to a variety of results concerning the rates of momentum and energy loss from the wave field by breaking and to statistical properties of the wave field such as the average frequency with which the surface turns over and the distribution of length of breaking front per unit surface area according to speed of advance of the breaking region. Limiting forms for the rates of energy and momentum loss have been guessed previously on dimensional grounds, but the expressions to be derived here exhibit specifically the interrelations among them and their dependence on the properties of waves in the equilibrium range and also provide some constraints on the numerical constants involved.

2. The statistical equilibrium among short waves

The two-dimensional wavenumber spectrum of a random distribution of surface waves is usually specified in terms of the covariance of the surface displacement ζ at points separated by a distance $\boldsymbol{r}$:

$$\Psi(\boldsymbol{k}) = (2\pi)^{-2} \int \overline{\zeta(\boldsymbol{x})\,\zeta(\boldsymbol{x}+\boldsymbol{r})}\, \mathrm{e}^{-\mathrm{i}\boldsymbol{k}\cdot\boldsymbol{r}}\, \mathrm{d}\boldsymbol{r}, \tag{2.1}$$

where the integral is over the entire $\boldsymbol{r}$-plane. From the inverse of the Fourier transform,

$$\overline{\zeta^2} = \int \Psi(\boldsymbol{k})\, \mathrm{d}\boldsymbol{k}, \tag{2.2}$$

where this integral is over the entire wavenumber plane. Note that, since the covariance is an even function of $\boldsymbol{r}$,

$$\Psi(\boldsymbol{k}) = \Psi(-\boldsymbol{k}). \tag{2.3}$$

The dynamics of the wave field is, however, more conveniently described (particularly when long-wave/short-wave interactions are involved, as they may be in the equilibrium range or when the waves are disturbed by currents) by the balance of action spectral density, defined as

$$\begin{aligned} N(\boldsymbol{k}) &= \frac{g}{\sigma}\, \Psi(\boldsymbol{k}), \\ &= \left(\frac{g}{k}\right)^{\frac{1}{2}} \Psi(\boldsymbol{k}), \end{aligned} \tag{2.4}$$

the latter form being pertinent to gravity waves, for which the intrinsic frequency $\sigma = (gk)^{\frac{1}{2}}$. In these expressions, the water density is divided throughout so that the air density is $\rho_{\mathrm{a}}/\rho_{\mathrm{w}}$. Following energy paths, the action spectral density is conserved except for the processes of action exchange among different wave groups by nonlinear

interactions, input from the wind and dissipation by wave-breaking, so that the balance of action spectral density can be represented (see e.g. Phillips 1977) as

$$\frac{\mathrm{d}N}{\mathrm{d}t} = \frac{\partial N}{\partial t} + (\boldsymbol{c}_g + \boldsymbol{U})\cdot\boldsymbol{\nabla} N = -\boldsymbol{\nabla}_{\boldsymbol{k}}\cdot\boldsymbol{T}(\boldsymbol{k}) + S_{\mathrm{w}} - D. \tag{2.5}$$

In this equation $\boldsymbol{T}(\boldsymbol{k})$ represents the net spectral flux of action through the wavenumber $\boldsymbol{k}$ by resonant wave–wave interactions, and the flux divergence in wavenumber space represents the net gain or loss of action spectral density at the wavenumber $\boldsymbol{k}$. These spectral exchanges are conservative for gravity waves, so that the integral of the first term on the right of (2.5) vanishes. The rates of spectral input from the wind S_{w} and loss D by breaking or by the formation of parasitic capillaries are represented only schematically in this equation. Their detailed forms will be considered later.

As a wave field develops under the continued action of the wind, the dominant waves become more energetic and longer, but for the components whose wavenumbers are large compared with that of the spectral peak, the timescales of their *growth* becomes large compared with their internal timescales involved with wave–wave interactions, action input from the wind and loss by breaking. Consequently, these components approach a state of statistical equilibrium determined by a balance among these last three processes:

$$-\boldsymbol{\nabla}_{\boldsymbol{k}}\cdot\boldsymbol{T}(\boldsymbol{k}) + S_{\mathrm{w}} - D = 0. \tag{2.6}$$

In this equilibrium range, the detailed functional form of each of these terms is expected to depend on the nature of the spectrum $N(\boldsymbol{k})$ in this range and it is of interest to enquire what spectral characteristics are associated with the possible balances among the three terms of (2.6).

A recent study by Komen, Hasselmann & Hasselmann (1984) has examined the balances among these processes in a 'fully developed' sea in the vicinity of the spectral peak and to frequencies up to 2.5 times that of the peak. The range of wavenumbers covered by these numerical calculations hardly extends into the equilibrium range, and the expressions they assume for the wind input is accurate only for wave components travelling faster than about $10u_*$ (as is seen in more detail below), but these calculations do give valuable insights into the balances to be expected in this region of the spectrum. They are almost certainly more complex than those deep in the equilibrium range itself; our primary concern is with wavenumbers that are large compared with those of the spectral peak and the balances (2.6) that obtain over *these* wavenumbers even if the longer waves are still developing.

First, let us consider the spectral redistribution of wave action which has been the subject of pioneering investigations by Hasselmann (1962, 1963) and others. It can be represented as a 'collision integral' over sets of four resonantly interacting gravity waves:

$$-\boldsymbol{\nabla}_{\boldsymbol{k}}\cdot\boldsymbol{T}(\boldsymbol{k}) = \iiint Q^2\{[N(\boldsymbol{k}) + N(\boldsymbol{k}_1)]\,N(\boldsymbol{k}_2)\,N(\boldsymbol{k}_3) - [N(\boldsymbol{k}_2) + N(\boldsymbol{k}_3)]\,N(\boldsymbol{k})\,N(\boldsymbol{k}_1)\}$$
$$\times\,\delta(\boldsymbol{k}+\boldsymbol{k}_1-\boldsymbol{k}_2-\boldsymbol{k}_3)\,\delta(\sigma+\sigma_1-\sigma_2-\sigma_3)\,\mathrm{d}\boldsymbol{k}_1\,\mathrm{d}\boldsymbol{k}_2\,\mathrm{d}\boldsymbol{k}_3, \tag{2.7}$$

where the coupling coefficient Q is a complicated homogeneous function of the wavenumbers $\boldsymbol{k}, \ldots, \boldsymbol{k}_3$ and is of order k^3. The Dirac delta function δ selects out those components obeying the resonance conditions for weak gravity-wave interactions

$$\boldsymbol{k} + \boldsymbol{k}_1 = \boldsymbol{k}_2 + \boldsymbol{k}_3, \quad \sigma + \sigma_1 = \sigma_2 + \sigma_3,$$

and the integral is cubic rather than quadratic in N because resonant gravity-wave interactions involve sets of four components, rather than three, as in most other wave types. Extensive calculations by Sell & Hasselmann (1972), Fox (1976) and Longuet-Higgins (1976) indicate that the dominant interactions are primarily local in the wavenumber plane at the relatively small wave slopes encountered in natural field wind-wave systems; Q is largest when the four wavenumbers concerned are all comparable (i.e. within a factor of two or so) in magnitude and, incidentally, in direction. Consequently, the net action transfer to a given wavenumber interval is determined primarily by the action spectral density in this vicinity. Near the spectral peak, of course, the flux to neighbouring wavenumbers is dominated by the presence of the peak itself, but at *wavenumbers large compared with that of the peak*, in the equilibrium range, the net spectral flux divergence at wavenumber $\boldsymbol{k}$ is determined by the values of N in *this* region, which scale as the local value $N(\boldsymbol{k})$ itself. As a result, since (2.7) is cubic in N and since $Q^2 \propto k^6$, the net spectral flux divergence

$$-\nabla_{\boldsymbol{k}} \cdot \boldsymbol{T}(\boldsymbol{k}) \propto Q^2 N^3(\boldsymbol{k})\, k^4/\sigma,$$
$$\propto g^{-\frac{1}{2}} k^{\frac{19}{2}} N^3(\boldsymbol{k}), \tag{2.8}$$

for gravity waves, for which $\sigma = (gk)^{\frac{1}{2}}$. This form was given by Kitaigorodskii (1983).

Equation (2.8) can be expressed more neatly in terms of a dimensionless function, the degree of saturation

$$B(\boldsymbol{k}) = k^4\, \Psi(\boldsymbol{k}) = g^{-\frac{1}{2}} k^{\frac{9}{2}} N(\boldsymbol{k}) \tag{2.9}$$

defined by the author (1984). Under the old saturation-range assumption with the spectral form (1.1), $B(\boldsymbol{k})$ would be, at most, a function of θ, the angle between the wavenumber and the wind. However, as we have seen, this need not be so; in a dynamical equilibrium, B may also be a function of k, though one would anticipate that the dependence may be rather weak. In terms of the degree of saturation, (2.8) becomes

$$-\nabla_{\boldsymbol{k}} \cdot \boldsymbol{T}(\boldsymbol{k}) \propto g k^{-4} B^3(\boldsymbol{k}). \tag{2.10}$$

The rate of action (or energy) input from the wind has been the subject of many theoretical and experimental investigations over the past 20 years that have, if nothing else, demonstrated the complexity and variety of the detailed processes involved. In order to provide a robust expression for S_{w} in (2.6), the best guide seems to be provided by the careful analysis of experiments interpreted in the light of only very general theoretical considerations. Plant (1982) suggests from a survey of such measurements that

$$S_{\mathrm{w}} = m \cos\theta\ \sigma \left(\frac{u_*}{c}\right)^2 N(\boldsymbol{k}), \tag{2.11}$$

where he finds m to be about 0.04, u_* is the friction velocity of the air flow over the water surface and c the phase velocity of the component concerned. As illustrated in figure 1, this form is a reasonably accurate representation for those gravity-wave components for which $u_*/c > 0.1$ (for lower-frequency components it seems to be an overestimate), but waves for which $c < 10u_*$ include the equilibrium range even in well-developed oceanic situations. An expression of the form (2.11) has been suggested by others as well. Mitsuyasu & Honda (1982) give a numerical coefficient of 0.05, and Gent & Taylor's (1976) calculation suggests $m \sim 0.07$, but it will be seen later that these larger values seem inconsistent with measurements of other quantities.

One might indeed expect a spectral action input rate of the form (2.11) on general

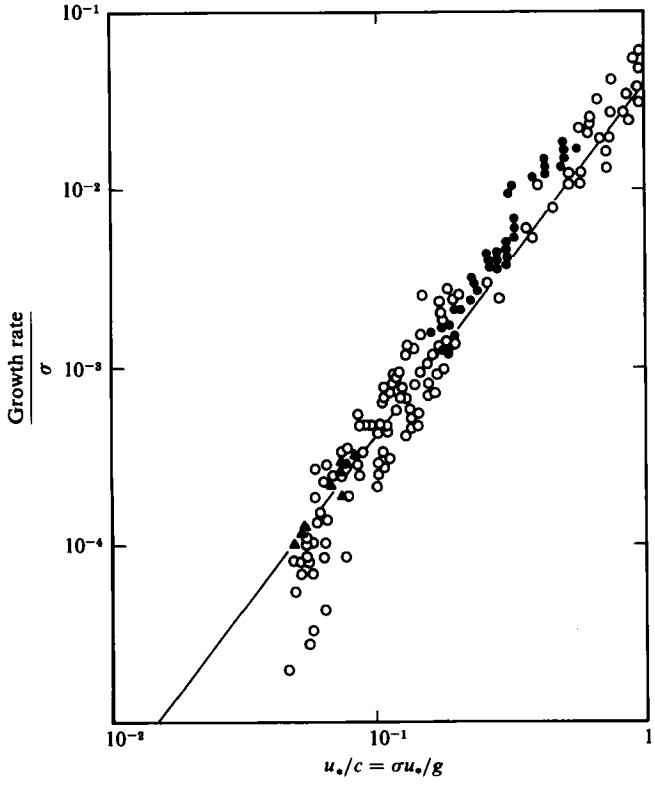

FIGURE 1. Measurements of the growth rate divided by radian frequency in terms of u_*/c. The open circles represent data surveyed by Plant (1982), the solid circles are measurements by Mitsuyasu & Honda (1982) and the triangles by Schule *et al.* (1971).

dynamical grounds. The critical layers associated with waves whose phase speeds are less than $10u_*$ have disappeared into the region, ill-defined aerodynamically, of the viscous sublayer just above the water surface or among the roughness elements produced by very short capillary waves. (Only for the longer wave components, for which c is adequately larger than $10u_*$, is the critical layer clear of the water surface, so that the rightly celebrated Miles (1957) mechanism becomes effective.) At the shorter scales, the energy transfer occurs by direct variations in surface stress, both normal and tangential. The mean wind stress $\tau = (\rho_a/\rho_w)\, u_*^2$, in units normalized by the water density, is disturbed by flow over waves with slope ak, so that the first-order perturbations in stress are proportional to $(\rho_a/\rho_w)\, u_*^2\, ak$. If wind and waves are not moving in the same direction, one might argue that to the first order only the stress component normal to the wave crests is perturbed, so that the magnitude of the stress variations, normal and tangential, is proportional to $(\rho_a/\rho_w)\, u_*^2\, ak \cos\theta$. The rate of doing work on the water surface is the mean scalar product of the stress variations across the surface and the orbital velocity, with magnitude $(ak)c$, i.e. $(\rho_a/\rho_w) \cos\theta\, u_*^2\, (ak)^2 c$. Since Ψ is the spectrum of the surface displacement, the spectral rate of energy input is

$$\frac{\rho_a}{\rho_w} \cos\theta\, u_*^2\, k^2 c \Psi(\boldsymbol{k}),$$

and the spectral rate of action input is this divided by the intrinsic frequency σ:

$$S_{\mathrm{w}} \propto \frac{\rho_{\mathrm{a}}}{\rho_{\mathrm{w}}} \cos\theta\, u_*^2 k^2 c\sigma^{-1} \Psi(\boldsymbol{k}),$$
$$= \frac{\rho_{\mathrm{a}}}{\rho_{\mathrm{w}}} \cos\theta \left(\frac{u_*}{c}\right)^2 \sigma N(\boldsymbol{k}),$$

from (2.4), which agrees with (2.11).

Although a specific directional factor appears in these expressions, it would be unwise at this stage to ascribe too much significance to it. In the measurements analysed by Plant (1982), θ was, in essence, zero. Even if the wind were perfectly steady, three-dimensional effects of the air flow over wave hummocks are not properly addressed in these arguments. Under natural conditions, an alert helmsman knows that, in a nominally steady wind, its direction as well as magnitude varies randomly on timescales that are for him and for short-wave generation, significant. Consequently, it seems more prudent to take

$$S_{\mathrm{w}} = m \cos^{2p}\theta\, \sigma \left(\frac{u_*}{c}\right)^2 N(\boldsymbol{k}), \tag{2.12}$$

where the value of p may be deduced from observational data. In terms of the degree of saturation defined earlier,

$$S_{\mathrm{w}} = m \cos^{2p}\theta\, g k^{-4} \left(\frac{u_*}{c}\right)^2 B(\boldsymbol{k}). \tag{2.13}$$

The development of an expression for the rate of spectral action dissipation has fewer antecedents. Hasselmann (1974) provided a specific model involving a distribution of small dissipation perturbations, but this seems hardly appropriate here. The key is to establish the functional dependence of the dissipation rate on the quantities involved in the specification of the equilibrium range; the specific form of the function is given by the need to preserve the equilibrium balance (2.6).

Wave-breaking is a local process in physical space, so a distributed process in Fourier space, and the occurrences of local wave-breaking and the consequent action and energy losses are the result of local excesses, however these excesses are produced. They may arise from a local convergence in an underlying current which increases the local degree of saturation and consequently the intensity of breaking. In an active wind-generated wave field where wave–current interactions are negligible, the degree of saturation may be enhanced by wind input, but the extent to which wave-breaking occurs and the rate of action or energy loss from wavenumber $\boldsymbol{k}$ still has as its primary causative property some functional of the degree of saturation B over a range of wavenumbers surrounding $\boldsymbol{k}$.† Now, in the equilibrium range, with a wide separation between its upper and lower wavenumber limits, there are no internal wavenumber scales, so that in this functional, whatever it is (provided that its range of integration concerns only the equilibrium range), the degree of saturation B at other wavenumbers scales with that of $\boldsymbol{k}$. The spectral rate of action dissipation can then be expressed

† It is possible, as Professor H. Mitsuyasu has suggested to me, that, in a very strong wind-generated situation with steep dominant waves, the average spectral density at wavenumbers in the equilibrium range may be suppressed by additional significant local spectral action losses near the dominant wave crests. The statement above may then remain true locally, but, to find the overall spectral density, one would have to consider the departures from local equilibrium resulting from the interactions with the steep long waves, and average over the result.

as a function, rather than a functional of $B(\boldsymbol{k})$. D has dimensions gk^{-4}, and if, for example,

$$D(\boldsymbol{k}) = gk^{-6} \int F(\boldsymbol{k}'/k, B(\boldsymbol{k}'))\, \mathrm{d}\boldsymbol{k}'$$

(remembering the L^{-2} dimension in $\mathrm{d}\boldsymbol{k}$), and anticipating that $B(\boldsymbol{k})$ varies as some power q of k, then

$$\begin{aligned} D &= gk^{-6} \int F\left(\frac{\boldsymbol{k}'}{k}, \left(\frac{k'}{k}\right)^q B(\boldsymbol{k})\right) \mathrm{d}\boldsymbol{k}', \\ &= gk^{-4} \int F(\boldsymbol{\kappa}, \kappa^q B(\boldsymbol{k}))\, \mathrm{d}\boldsymbol{\kappa}, \quad \text{where } \boldsymbol{\kappa} = \frac{\boldsymbol{k}'}{k}, \\ &= gk^{-4} f(B(\boldsymbol{k})), \end{aligned} \tag{2.14}$$

in accordance with the reasoning above.

These arguments give the functional dependence of the dissipation rate in the equilibrium range, but, as mentioned previously, not the form of the function f. From the formal mathematical point of view, this is determined simply by the need to close the equilibrium balance (2.6). Those who have struggled to find a spectral representation of wave dissipation may find this view somewhat uncomfortable, but it does, I believe, parallel the physics. The spectral dissipation of action or energy by wave-breaking in the equilibrium range occurs at whatever rate is needed to accommodate the net input. There is a close analogy here with the theory of turbulence at high Reynolds numbers: the rate of viscous dissipation by the small eddies is simply what is handed down to them from larger eddies as a result of the strong nonlinear interactions – their velocity and lengthscales (in this case) adjust themselves to accommodate whatever the spectral transfer provides.

It is important to emphasize again that the processes of wave–wave interaction and losses by wave-breaking are not, in general, spectrally local as, indeed, the calculations of Komen *et al.* (1984) demonstrate explicitly. Only over wavenumbers that are more distant both from the spectral peak and from the upper limit to this range than half the interval of wavenumbers that is needed to specify these non-local processes, that is, only well inside the equilibrium range, can these scaling arguments be used to represent them as, in effect, spectrally local.

In summary, then, we have three physical processes that are pertinent to the equilibrium range in an active wind-generated sea, that balance among themselves and are of the forms:

$$\left.\begin{aligned} &\text{spectral flux divergence} \propto gk^{-4} B^3(\boldsymbol{k}), \\ &\text{wind input} = m \cos^{2p}\theta\, gk^{-4} \left(\frac{u_*}{c}\right)^2 B(\boldsymbol{k}), \\ &\text{dissipation} = gk^{-4} f(B(\boldsymbol{k})). \end{aligned}\right\} \tag{2.15}$$

What is the nature of this balance? There are several alternatives.

Kitaigorodskii (1983) has proposed the existence of a Kolmogoroff-type equilibrium range in wind-generated waves in which the energy input from the wind is assumed to occur primarily at the energy-containing scales with dissipation restricted to much larger wavenumbers. This then postulates the existence of a range of wavenumbers over which the spectral flux divergence, wind input and dissipation rate are *all* negligible; the balance (2.6) is achieved by all terms vanishing. The directionally integrated spectral energy flux ϵ_0 is constant over this range. A critical step in his argument is that the spectral flux itself, like the flux divergence in (2.15), is cubic

in the spectral density, so that the directionally averaged spectrum $F(k)$ is proportional to $\epsilon_0^{\frac{1}{3}}$. With this basis, it then follows on similarity grounds that

$$F(k) = \int_{-\pi}^{\pi} \Psi(k, \theta)\, \mathrm{d}\theta \propto \epsilon_0^{\frac{1}{3}} g^{-\frac{1}{2}} k^{-\frac{7}{2}}. \tag{2.16}$$

The corresponding frequency spectrum, with the dispersion relation $\sigma = (gk)^{\frac{1}{2}}$, is

$$\Phi(\sigma) \propto \epsilon_0^{\frac{1}{3}} g \sigma^{-4}. \tag{2.17}$$

Arguing further that $\epsilon_0 \propto (\rho_a/\rho_w)\, U^3$, where U is the mean wind speed or, approximately, that $\epsilon_0 \propto u_*^3$, he obtains wavenumber and frequency spectra of the forms

$$\left.\begin{aligned} F(k) &\propto u_* g^{-\frac{1}{2}} k^{-\frac{7}{2}}, \\ \Phi(\sigma) &\propto u_* g \sigma^{-4}, \end{aligned}\right\} \tag{2.18}$$

the latter of which is precisely the form found empirically by Toba.

The principal conceptual difficulty with Kitaigorodskii's argument is the need to postulate that the energy input from the wind is concentrated at wavenumbers close to that of the spectral peak. To be sure, the air flow over the dominant waves may modify somewhat the rate of energy input to smaller waves, but it is difficult to see why it should be suppressed entirely. Indeed, according to (2.11), the rate of action input is, for $\theta \sim 0$,

$$\frac{S_w}{N(\boldsymbol{k})} \approx 0.04 \left(\frac{u_*}{c}\right)^2 \sigma = 0.04 g^{-2} u_*^2 \sigma^3,$$

which increases rapidly, rather than decreases, as the frequency increases. Direct measurements by Snyder *et al.* (1981) made in the Bight of Abaco, Bahamas, on the surface-pressure fluctuations in air flow over waves show also that the rate of energy input per wave cycle continues to increase with frequency up to the highest values they could measure, which corresponded to $c/u_* \sim 5$, well into the equilibrium range. Yet the main result of Kitaigorodskii's analysis does agree with the form proposed by Toba!

The object of this paper is to indicate how an equilibrium spectrum of the Toba type as well as other spectral forms can be derived from a very different assumption about the dynamical balances in the equilibrium range, and this, at the same time, allows us to derive (rather than infer from observations or postulate on dimensional grounds) a number of expressions concerning the energy and momentum flux that is supported by the equilibrium range and the statistical characteristics of the breaking events themselves. We have just seen that the experiments summarized by Plant (1982) over the range $0.5 < c/u_* < 10$ and those of the Bight of Abaco from $5 < c/u_* < 20$ or so indicate that direct energy transfer from the wind continues to be important throughout the equilibrium range. There are no direct measurements of the spectral flux divergence associated with nonlinear interactions, but the calculations summarized in the JONSWAP report (Hasselmann *et al.* 1973), or those given by Komen *et al.* (1984) indicate that it is negative (meaning a net energy input), and continues to be so over all frequencies calculated above twice that of the spectral peak, that is, in the equilibrium range. Although the actual magnitudes found are specific to the spectral forms used in the calculations, the consistency of this qualitative feature gives confidence that nonlinear action and energy spectral flux divergences remain an important characteristic of the equilibrium range. There are neither direct measurements nor reliable calculations concerning the spectral rate of

action and energy dissipation by breaking, but even a casual observation of the sea surface under active wind-generating conditions will note the occurrence of breaking events over a range of scales from longer, vigorous events associated often with the dominant waves, producing whitecapping, air entrainment and a trail of foam, through smaller, more transient events with splashing and a few air bubbles to much smaller breaking occurrences, microscale breaking (these need a quicker eye) in which rippling and possibly a train of parasitic capillaries indicate that the sea surface is turning over. It seems reasonable then to assume that these dissipative processes also are pertinent throughout the equilibrium range.

Let us therefore explore the consequences of the assumption that, *in the equilibrium range, the processes of energy input from the wind, spectral flux divergence and loss by breaking are all of importance*, and that the balance (2.6) includes non-trivial contributions from all three. Now, at wavenumbers inside the equilibrium range, those substantially larger than that of the spectral peak and much smaller than those influenced by capillarity, molecular viscosity or drift of the surface skin, the local dynamical balance is, as argued previously, uninfluenced by wave characteristics outside this spectral range. The equilibrium range has no *internal* wavenumber scale (except for the wavenumber under consideration) so that the *ratios* of the terms in the spectral action balance must be constant. (If there *were* some internal wavenumber scale, k_s say, then the ratios at wavenumber k could be a function of k/k_s, but this is not so.) Consequently, well inside the equilibrium range, though not at wavenumbers near the spectral peak nor near the upper wavenumber limit, all three quantities in (2.15) must be proportional, and

$$B^3(\boldsymbol{k}) \propto m \cos^{2p}\theta \left(\frac{u_*}{c}\right)^2 B(\boldsymbol{k}) \propto f(B(\boldsymbol{k})). \tag{2.19}$$

It follows immediately that the degree of saturation

$$B(\boldsymbol{k}) = \beta \cos^p\theta \left(\frac{u_*}{c}\right), \tag{2.20}$$

and the dimensionless action dissipation function

$$f(B) = \gamma B^3(\boldsymbol{k}), \tag{2.21}$$

where β and γ are numerical constants. (Note that, from the definitions, $B(\boldsymbol{k}) = B(-\boldsymbol{k})$; in (2.20) the absolute value of $\cos\theta$ is to be understood.)

3. Wave spectra in the equilibrium range

Equations (2.20) and (2.9) lead to a wavenumber spectrum in the equilibrium range of the form

$$\begin{aligned} \Psi(\boldsymbol{k}) &= k^{-4} B(\boldsymbol{k}), \\ &= \beta(\cos\theta)^p \left(\frac{u_*}{c}\right) k^{-4}, \\ &= \beta(\cos\theta)^p u_* g^{-\frac{1}{2}} k^{-\frac{7}{2}}, \end{aligned} \tag{3.1}$$

over a range of wavenumbers substantially larger than that of the spectral peak. The upper limit in wavenumber to which this range can be expected to extend is determined by the smallest wavenumber at which new, small-scale dynamical effects become important. These may include capillarity, molecular viscosity or dissipation in surface films or the suppression of very short gravity waves by surface drift; these dynamical limitations will be considered in detail shortly.

The frequency spectrum in the equilibrium range can be found from (3.1) by integration over all wavenumbers at constant frequency σ. The use of the dispersion relation $\sigma = (gk)^{\frac{1}{2}}$ neglects the Doppler-shifting from the oscillatory advection of short waves by the orbital velocities of the dominant waves (or by tidal currents, if they are present) and places a kinematic upper limit to the range of frequencies that is distinct from, and generally more restrictive than, the dynamical limitations mentioned in the previous paragraph. If $\overline{\zeta^2}$ is the mean-square surface displacement in the wave field associated with the dominant waves, the corresponding orbital speeds are of order $2(\overline{\zeta^2})^{\frac{1}{2}}\sigma_0$, where σ_0 is the peak frequency. The Doppler-shifting is insignificant only for those components whose intrinsic phase speed g/σ is large compared to this, or whose frequencies are less than

$$\frac{g}{2(\overline{\zeta^2})^{\frac{1}{2}}\sigma_0} = (4\pi s)^{-1}\sigma_0, \tag{3.2}$$

where $s = (\overline{\zeta^2})^{\frac{1}{2}}/\lambda_0$, the so-called 'significant slope' of Huang *et al.* (1981), λ_0 being the dominant wavelength. Accordingly, the frequency spectrum

$$\begin{aligned}\Phi(\sigma) &= 2\int_{-\frac{1}{2}\pi}^{\frac{1}{2}\pi} k\Psi(\boldsymbol{k})\left(\frac{\partial\sigma}{\partial k}\right)^{-1}\mathrm{d}\theta\Big|_{k=\sigma^2/g}, \\ &= 4\beta I(p)\,u_*\,g\sigma^{-4}, \qquad (3.3)\\ &= \alpha u_*\,g\sigma^{-4} \quad \text{when } \sigma_0 \ll \sigma \ll (4\pi s)^{-1}\sigma_0, \qquad (3.4)\end{aligned}$$

where

$$I(p) = \int_{-\frac{1}{2}\pi}^{\frac{1}{2}\pi} (\cos\theta)^p\,\mathrm{d}\theta = B(\tfrac{1}{2}, \tfrac{1}{2}(p+1)), \tag{3.5}$$

in terms of the beta function $B(m, n)$. The variation of this integral with p is illustrated in figure 2.

These spectra (3.1) and (3.4) are similar to those derived by Kitaigorodskii (1983) on a quite different dynamical basis, though his theory gives only the directionally averaged version of (3.1). Why the similarity? A key ingredient in both theories is the cubic dependence on the spectral density of the spectral-flux divergence (here) and the spectral flux itself (in Kitaigorodskii's approach). Kitaigorodskii assumes that the directionally integrated energy spectral flux, independent of k, is proportional to u_*^3, so that the spectral density is proportional to u_* – the rest follows by dimensional analysis. In the present approach, the action spectral-flux divergence is proportional to $gk^{-4}B^3(\boldsymbol{k})$ so that the energy spectral-flux divergence $\nabla_{\boldsymbol{k}}\cdot\epsilon(\boldsymbol{k})$ is σ times this, or

$$\nabla_{\boldsymbol{k}}\cdot\epsilon(\boldsymbol{k}) \propto -(\cos\theta)^{3p}\,u_*^3\,k^{-2}, \tag{3.6}$$

from (2.20), which has the same u_*^3 dependence. Since this flux divergence plays a central part in the balance (2.6) or (2.15) underlying this theory, as does the spectral flux itself (assumed constant) in Kitaigorodskii's theory, then, for dimensional reasons, the results must be equivalent, at least as far as the spectral shapes are concerned.

Many more measurements are available of the frequency spectrum than of the wavenumber spectrum, though in reviewing them one must be alert to distortions at higher frequencies introduced by Doppler-shifting. Most of the spectra that, as an ensemble, suggested a σ^{-5} form for the equilibrium range (Phillips 1977), were measured at various wind speeds and averaged directly (in dimensional form rather than in the dimensionless form of figure 3) and it is difficult to reanalyse them. More recent, better documented and better analysed field measurements have been made

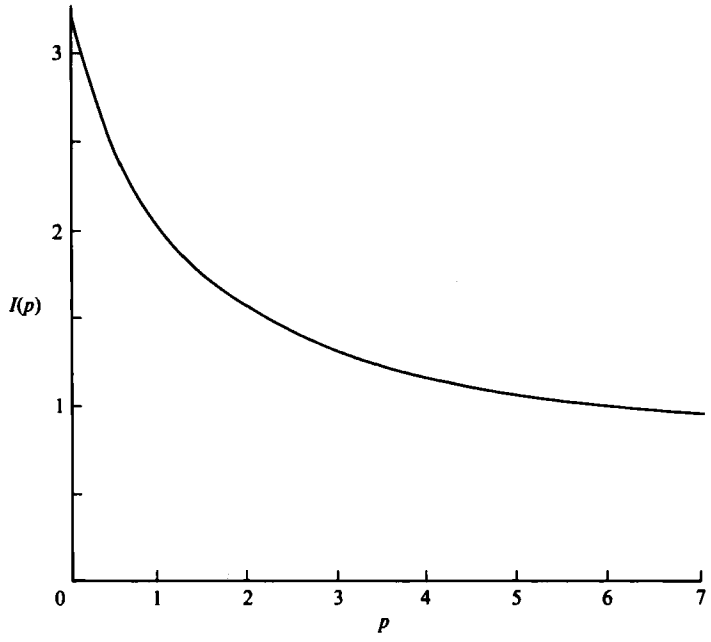

FIGURE 2. The integral $I(p)$ of (3.8) as a function of p.

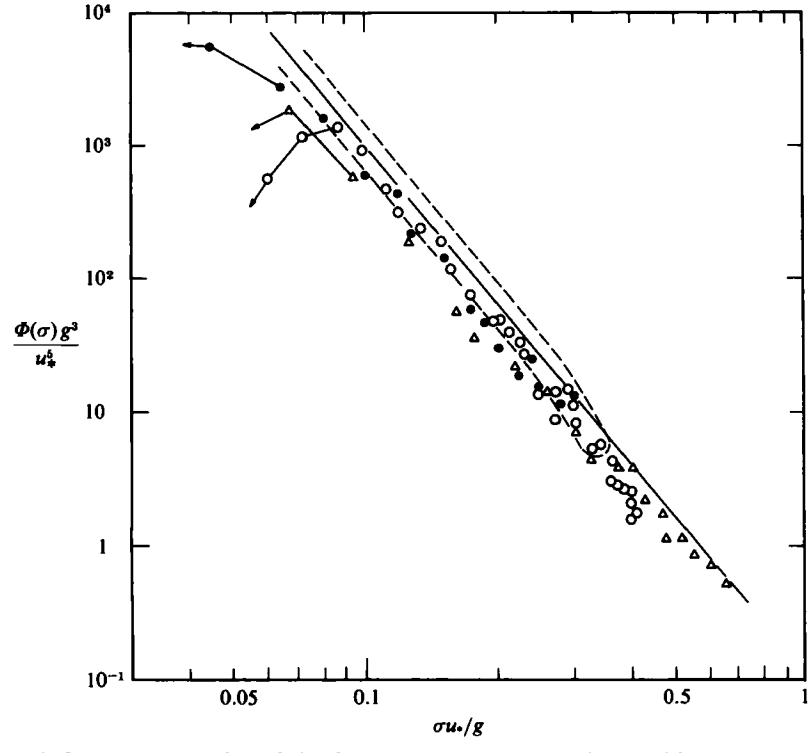

FIGURE 3. A dimensionless plot of the frequency spectrum in the equilibrium range. The broken lines enclose the extensive measurements of Forristall (1981) and the continuous line represents (3.4) with $\alpha = 0.11$. The open circles indicate results from Kawai *et al.* (1977) at $u_* = 37.2$ cm/s; results from Kondo *et al.* (1973) are shown as solid circles at $u_* = 49.6$ cm/s and the triangles at $u_* = 24.4$ cm/s.

Author	Number of spectra	α ($\times 10^{-2}$)	gx/U_{10}^2 ($\times 10^3$)	$\sigma_0 u_*/g$ ($\times 10^{-2}$)	s ($\times 10^{-2}$)
Laboratory					
Toba (1973)	—	2	$c(2\times 10^{-4})$	70–130	~ 5
Field					
Kondo *et al.* (1973)	2	6	—	2–5	—
Kawai *et al.* (1977)	54	6.2 ± 0.1	0.2–2	2–9	1–2
Mitsuyasu *et al.* (1980)	14	8.7	5–100	2–7	0.8–2
Kahma (1981)	*ca.* 50	11	0.5–6	1.5–6	—
Forristall (1981)	Many	11.0	—	2–6	0.8–2

TABLE 1. A summary of measurement values of Toba's constant α, with the ranges of dimensionless fetch gx/U_{10}^2, dimensionless frequency of the dominant wave $\sigma_0 u_*/g$ and 'significant slope' s of the dominant waves

by Kawai *et al.* (1977), Mitsuyasu *et al.*(1980), Forristall (1981) and Kahma (1981): some of these are summarized in figure 3 and table 1. The individual sets of measurements all indicate slopes close to -4, but the scatter in spectral level (that is, the value of Toba's constant α) is considerably greater among the different sets than it is within each individual set. There seem to be no systematic variations with 'significant slope' s over this range or with gx/U_{10}^2 or $\sigma_0 u_*/g$, but the values found by the Japanese investigators are lower than those from the North American studies. The waves themselves should be pretty much the same in both Hemispheres, but there may be some systematic calibration or analysis differences. The spectrum of Kawai *et al.* shown is only one of 54 measured; in their series individual spectra had a mean slope and standard deviation of 4.13 ± 0.20, the constant α in (3.4) being 0.062 ± 0.010. Forristall's data, taken from offshore platforms, cover a wide range of meteorological conditions including hurricanes, U.S. East Coast winter storms as well as relatively mild conditions in the Gulf of Mexico, but nonetheless they group quite tightly around a line proportional to $(\sigma u_*/g)^{-4}$, tailing off to a slightly higher slope, about $(\sigma u_*/g)^{-5}$, when $\sigma u_*/g > 0.2$. His mean value for the Toba constant is given as 0.110 (after recalculation of frequencies from Hz to rad/s). Toba's earlier laboratory results at large values of $\sigma_0 u_*/g = u_*/c_0$ give α a good bit smaller than the field values, but they are almost certainly influenced strongly by wind-drift effects. As far as the frequency spectrum is concerned, then, there seems to be little question that (3.4) agrees better with a wide range of field data than does (1.2), though some unfortunate uncertainty persists concerning the precise value of α. Nevertheless, the theory developed in this paper will offer some constraints that may somewhat reduce this uncertainty.

The two-dimensional wavenumber spectrum $\Psi(\boldsymbol{k})$ contains more information than the frequency spectrum and is more directly interpreted, since the wavenumber distortions of the equilibrium range produced by dominant wave straining are smaller (proportional to ak) than the Doppler-shifting in the frequency spectrum (proportional to $(\sigma/\sigma_0)ak$. The pioneering measurements of Pierson (1962) in the Stereo Wave Observation Project provide what is still the most direct measurement of $\Psi(\boldsymbol{k})$, though the data is limited and the accuracy not high. There have been, of course, a number of directional frequency spectra, and these will be discussed later. Remote sensing by radar observations has to date been more successful in measuring the spectra of swell (Beal *et al.* 1981) than of the shorter, equilibrium-range components.

There are, however, a number of measurements that can be related directly to the wavenumber spectrum $\Psi(\boldsymbol{k})$. The wavenumber spectrum of slope in the 1-direction, say,

$$\begin{aligned} S_{11}(\boldsymbol{k}) &= (2\pi)^{-2} \int \overline{\frac{\partial \zeta(\boldsymbol{x})}{\partial x_1} \frac{\partial \zeta(\boldsymbol{x}')}{\partial x_1'}} \, \mathrm{e}^{-\mathrm{i}\boldsymbol{k}\cdot\boldsymbol{r}} \, \mathrm{d}\boldsymbol{r}, \\ &= k_1^2 \, \Psi(\boldsymbol{k}), \end{aligned} \tag{3.7}$$

where $\boldsymbol{x}' = \boldsymbol{x} + \boldsymbol{r}$, and, if this direction is inclined at an angle θ_0 to the wind, the equilibrium-range form gives

$$S_{11}(\boldsymbol{k}) = \beta \{\cos(\theta - \theta_0)\}^p \cos^2\theta \, u_* g^{-\frac{1}{2}} k^{-\frac{3}{2}}. \tag{3.8}$$

The spectrum of the total slope,

$$\begin{aligned} S(\boldsymbol{k}) &= S_{11}(\boldsymbol{k}) + S_{22}(\boldsymbol{k}), \\ &= \beta \{\cos(\theta - \theta_0)\}^p \, u_* g^{-\frac{1}{2}} k^{-\frac{3}{2}}. \end{aligned} \tag{3.9}$$

Also, the spectrum of an instantaneous line traverse of the sea surface, the Fourier transform of $\overline{\zeta(\boldsymbol{x})\,\zeta(\boldsymbol{x}+r_1)}$, is

$$\chi(k_1) = \int_{-\infty}^{\infty} \Psi(\boldsymbol{k}) \, \mathrm{d}k_2, \tag{3.10}$$

and for wavenumbers k_1 in the equilibrium range, since $k_2 = k_1 \tan\theta$,

$$\begin{aligned} \chi(k_1) &= \beta u_* g^{-\frac{1}{2}} \int_{-\infty}^{\infty} \cos^p(\theta - \theta_0) \, (k_1^2 + k_2^2)^{-\frac{7}{4}} \, \mathrm{d}k_2, \\ &= \beta u_* g^{-\frac{1}{2}} k_1^{-\frac{5}{2}} \int_{-\frac{1}{2}\pi}^{\frac{1}{2}\pi} \cos^p(\theta - \theta_0) \cos^{\frac{3}{2}}\theta \, \mathrm{d}\theta. \end{aligned} \tag{3.11}$$

For a traverse in the windward direction, $\theta_0 = 0$ and

$$\chi(k_1) = I(p + \tfrac{3}{2}) \beta u_* g^{-\frac{1}{2}} k_1^{-\frac{5}{2}},$$

while, in the crosswind direction, $\theta_0 = \frac{1}{2}\pi$ and

$$\chi(k_1) = B(\tfrac{1}{2}(p+1), \tfrac{5}{4}) \beta u_* g^{-\frac{1}{2}} k_1^{-\frac{5}{2}},$$

where $B(m, n)$ is the beta function as usually defined. Three individual spectra of this kind were obtained with a laser wave profiler by Schule, Simpson & DeLeonibus (1971); they are shown in figure 4.11 of Phillips (1977). Overall, it must be admitted that these decrease at a rate more like k_1^{-3} (as predicted under the old saturation hypothesis) than $k_1^{-\frac{5}{2}}$. It would be very useful to repeat and extend measurements of this kind.

Another group of spectral forms can be related to the basic wavenumber spectrum only by the use of a dispersion relation, and this restricts their easy interpretability to frequencies for which long-wave Doppler-shifting is negligible. Foremost among these is the directional frequency spectrum

$$\Phi(\sigma, \theta) = \left[k \Psi(\boldsymbol{k}) \left(\frac{\partial \sigma}{\partial k} \right)^{-1} \right]_{k = \sigma^2/g}, \tag{3.12}$$

which is such that

$$\overline{\zeta^2} = \int_0^{\infty} \int_0^{2\pi} \Phi(\sigma, \theta) \, \mathrm{d}\theta \, \mathrm{d}\sigma.$$

(The spectrum $\Psi_0(\sigma,\theta)$ defined by Phillips (1977) is σ^{-1} times $\Phi(\sigma,\theta)$.) From (3.1) we have for the directional frequency spectrum

$$\Phi(\sigma,\theta) = 2\beta \cos^p\theta\, u_* g\sigma^{-4}. \tag{3.13}$$

Measurements of this spectrum have been made by Longuet-Higgins, Cartwright & Smith (1963) and Mitsuyasu *et al.* (1975, 1980) using different cloverleaf buoys. The angular distribution functions were found in both cases to be generally unimodal and broader for the higher frequencies of the equilibrium range than for frequencies near the spectral peak, though the angular resolution was limited. Donelan *et al.* (1984), with an array of 14 wave staffs in Lake Ontario, were able to confirm that the linear dispersion relation was obeyed to frequencies beyond three times that of the spectral peak, and that the frequency spectrum in the equilibrium range varied as σ^{-4}. Their study was concerned primarily with the directionality of longer-wave components, those in the vicinity of the spectral peak, but they found that, when $\sigma > 1.6\sigma_0$, the directional factor could be represented empirically as $\mathrm{sech}^2(1.24\theta)$. There is not much to choose (within the accuracy of the experiment) between this and a $(\cos\theta)^p$ distribution, with $p \sim 2$.

Finally, the frequency spectrum of slope, measured at a fixed point, can be expressed in terms of the wavenumber spectrum, but, since short gravity waves (and possibly capillary waves as well, which we do not consider in this paper) contribute substantially, the limitations imposed by Doppler-shifting are even more severe. Only the lower-frequency component of the slope spectrum can be calculated simply from the wavenumber spectrum; i.e., in a tidal stream with speed U, only for frequencies less than the minimum of $(4\pi s)^{-1}$ and g/U. Over this range, however, the frequency spectrum of slope in the windward direction

$$\begin{aligned} S_{11}(\sigma) &= 2\int_{-\frac{1}{2}\pi}^{\frac{1}{2}\pi} kS_{11}(\boldsymbol{k})\left(\frac{\partial\sigma}{\partial k}\right)^{-1} \mathrm{d}\theta\Big|_{k=\sigma^2/g}, \\ &= 4\beta I(p+2)\, u_* g^{-1}, \end{aligned} \tag{3.14}$$

from (2.8) with $\theta_0 = 0$. The corresponding spectrum of slope in the crosswind direction is found to be

$$S_{22}(\sigma) = 4\beta\{I(p) - I(p+2)\}\, u_* g^{-1}, \tag{3.15}$$

and the frequency spectrum of total slope in this range is

$$\begin{aligned} S(\sigma) &= S_{11}(\sigma) + S_{22}(\sigma), \\ &= 4\beta I(p)\, u_* g^{-1}, \\ &= \alpha u_* g^{-1}. \end{aligned} \tag{3.16}$$

These results indicate that the frequency spectra of slope are proportional to u_* and flat, independent of σ, provided the frequency is sufficiently smaller than those influenced by the convective effects of the longer waves or of any tidal stream. The well-known laboratory measurements of Cox (1958) do not have a discernible equilibrium spectral range among the gravity-wave components, but more recent field measurements by Tang & Shemdin (1983) do extend to much lower frequencies. Their results for the spectrum S_{11}, replotted according to (3.14), are shown in figure 4. These spectra were measured in the presence of waves with significant heights up to 1.23 m and tidal currents up to 0.6 m/s; in the low-wind case the range of validity of the dispersion-relation transformation was limited by tidal currents and in the others by long-wave advection. In each case, however, it appears that the kinematic advection effects had become serious at frequencies about 15 rad/s, so that the spectra can be

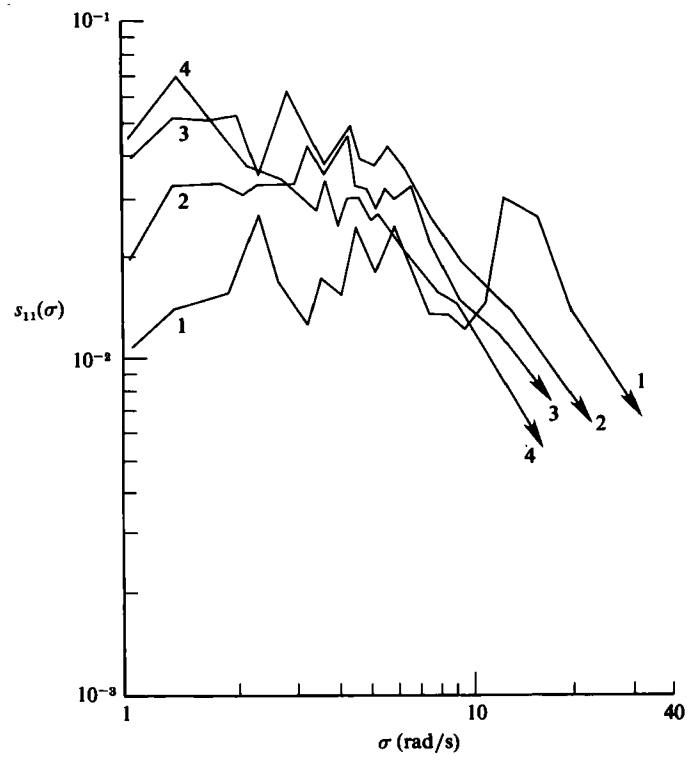

FIGURE 4. Frequency spectra of slope in the upwind, downwind direction measured by Tang & Shemdin (1983), rescaled according to (3.14). Curve 1 is at $u_* = 11$ cm/s; for 2, $u_* = 27$ cm/s; for 3, $u_* = 28$ cm/s; and, for 4, $u_* = 45$ cm/s.

compared with these results only over a frequency range substantially below this limit. The dynamical limitations (capillarity, and the influence of wind drift) become important only at higher frequencies in these experiments. Over the low-frequency range there is a good deal of sampling error, but not much systematic trend in the spectral levels below about 7 rad/s. The spectral densities measured in this range are generally consistent with the values obtained for Toba's constant:

$$4\beta I(p+2) = \frac{\alpha I(p+2)}{I(p)} < \alpha,$$

if α lies in the range 6×10^{-2} (Kawai *et al.*) to 11×10^{-2} (Forristall). At higher frequencies, where advection effects are significant and interpretation is difficult, the spectra measured clearly do not follow the form (3.14), but decrease approximately as σ^{-1}. The total mean-square slopes are not, of course, affected by the spectral distribution: Tang & Shemdin found that the downwind and transverse mean-square slopes were about equal in cases of a wind-wave field with a single well-defined peak.

4. Fluxes through the equilibrium range

An important aspect of the present theory is that it provides not only spectral forms in the equilibrium range, but also estimates for the spectral distributions and total rates of dissipation of wave action, wave energy and wave momentum, and these lead

to a variety of expressions that can be compared with existing observations or can suggest new ones.

The spectral rate of dissipation of wave action is given from (2.15), (2.20) and (2.21) as

$$\begin{aligned} D(\boldsymbol{k}) &= \gamma g k^{-4} B^3(\boldsymbol{k}), \\ &= \gamma \beta^3 (\cos\theta)^{3p} g k^{-4} \left(\frac{u_*}{c}\right)^3, \\ &= \gamma \beta^3 (\cos\theta)^{3p} g^{-\frac{1}{2}} u_*^3 k^{-\frac{5}{2}}. \end{aligned} \tag{4.1}$$

More interesting is the spectral rate of energy loss from the wave components in the equilibrium range:

$$\epsilon(\boldsymbol{k}) = \sigma D(\boldsymbol{k}) = \gamma \beta^3 (\cos\theta)^{3p} u_*^3 k^{-2}, \tag{4.2}$$

which is, of course, proportional to the spectral rate of energy input from the wind

$$\epsilon_{\mathrm{w}}(\boldsymbol{k}) = \sigma S_{\mathrm{w}} = m\beta (\cos\theta)^{3p} u_*^3 k^{-2},$$

from (2.15) and (2.20), but greater than it if the spectral flux divergence represents a net gain, as the JONSWAP calculations suggest. Consequently

$$\gamma\beta^2 > m \approx 0.04. \tag{4.3}$$

The expression (4.2) represents the spectral distribution of the rate of energy loss from the surface waves with wavenumber $\boldsymbol{k}$. The turbulence generated in the water as the result of wave-breaking has a lengthscale closer to that of the breaking zone than the wavelength, but, as we shall see later, the two are approximately proportional. Consequently, the energy source for the near-surface turbulence represented by wave-breaking is, in mean, distributed over a wide range of scales (the distribution over *scalar* wavenumber k being proportional to $u_*^3 k^{-1}$) rather than being concentrated at the energy-containing scales as it is in shear-generated turbulence. The energy supply is, however, highly intermittent, being associated with sporadic breaking events. Infrequent but large energy pulses at the larger scales and the much more frequent, smaller turbulent-energy pulses from small-scale breaking all contribute to the turbulent-energy supply. Turbulent-energy levels and local rates of dissipation are expected to be equally intermittent.

The spectral distribution of the mean flux of momentum transferred by breaking waves to the underlying water is given by

$$\begin{aligned} \tau(\boldsymbol{k}) &= \frac{\epsilon(\boldsymbol{k})}{c} \cos\theta, \\ &= \gamma \beta^3 (\cos\theta)^{3p+1} g^{-\frac{1}{2}} u_*^3 k^{-\frac{3}{2}}. \end{aligned} \tag{4.4}$$

The integral of this represents, of course, only that part of the mean momentum flux from the wind to the sea which is transferred to waves and subsequently lost by wave-breaking. Some part is transferred directly by the mean shear stress on the water surface and part, transferred to waves, is associated with wave growth. It may, however, represent a dominant part, as the considerations of §5 suggest. Part of the momentum flux (4.4) is supplied by transfer from the dominant waves near the spectral peak, so that the net rate of loss in the equilibrium range is greater than the net direct rate of energy input from the wind, in accordance with the inequality (4.3).

Expressions for the total rate of energy and momentum loss from the waves in the equilibrium range involve the values of the wavenumbers at the upper and lower limits of this range. Measurements of the frequency spectra in the field in an actively generated wave system indicate that the lower limit k_0 is surprisingly close to, but

rather above, the wavenumber of the spectral peak, the components concerned having just settled down from the overshoot effect. (Laboratory measurements are often dominated by harmonics of the primary wave, and the whole wave field is much less dispersive – see e.g. Ramamonjiarisoa & Coantic (1976) and Phillips (1981)). The upper limit k_1 to the equilibrium range is less certain. The kinematic distortions introduced by long-wave straining are only of order s in the wavenumber spectrum and can be neglected. The dynamical processes underlying this theory are specific to gravity waves, so that necessarily $k_1 \ll (g/\gamma)^{\frac{1}{2}}$, where γ is the ratio of surface tension to water density. More restrictive, however, is likely to be the effect of surface drift in the upper few millimetres of the water below the surface. Banner & Phillips (1974) have shown that, if the drift at the surface is q, then freely travelling gravity waves whose phase speed in this direction is less than q are strongly suppressed. A number of sets of observations, beginning with Keulegan (1951), have shown that $q \approx u_*$, so that if this suppression is effective in field situations then $k_1 \approx g/u_*^2$. This wavenumber lies in the gravity-wave range for all but the lightest winds and decreases as the wind speed increases. If wavenumbers above this value *are* suppressed, we are led to the rather uncomfortable conclusion that at higher wind speeds there is something of a spectral gap between the shortest freely travelling gravity waves of the equilibrium range and the capillary waves, which may be directly wind-generated, exist as parasitic capillaries or be generated by small-scale breaking. This would not, of course, be evident in the frequency spectra because of long-wave Doppler-shifting, and no wavenumber spectra yet exist that could resolve it. However, one's qualitative impression of looking at storm seas is that, despite streaks of foam and impressive dominant waves, the shorter gravity-wave roughnesses on the surface do not seem to be as distinct as they are under less violent conditions. A more persuasive reason will appear in a moment, and, if such a spectral gap does exist, it has important implications for remote sensing of the sea surface by radar wavelengths in this range.

In any event, the total rate of energy input into the surface-layer turbulence by wave-breaking over the equilibrium range is found by integration of (4.2):

$$\begin{aligned} \epsilon_0 &= 2\int_{-\frac{1}{2}\pi}^{\frac{1}{2}\pi}\int_{k_0}^{k_1} \epsilon(\boldsymbol{k})\, k\, \mathrm{d}k\, \mathrm{d}\theta, \\ &= 2\gamma\beta^3 I(3p)\, u_*^3 \ln\frac{k_1}{k_0}. \end{aligned} \tag{4.5}$$

Quantities such as this are more usually expressed in terms of the air density; restoring the density factors, we have

$$\epsilon_0 = \left(2\gamma\beta^3 I(3p)\frac{\rho_\mathrm{w}}{\rho_\mathrm{a}}\right)\rho_\mathrm{a}\, u_*^3 \ln\frac{k_1}{k_0}. \tag{4.6}$$

As a wave field develops from, say, an initial state of rest, the rate of energy transfer from waves to turbulence in the water, initially zero, increases logarithmically as the extent of the equilibrium range increases. If $k_1 = rg/u_*^2$ and we approximate k_0 by the wavenumber of the spectral peak, g/c_0^2, where r is a number approximately unity,

$$\epsilon_0 \approx \left(2\gamma\beta^3 I(3p)\frac{\rho_\mathrm{w}}{\rho_\mathrm{a}}\right)\rho_\mathrm{a}\, u_*^3 \ln\left[r\left(\frac{c_0}{u_*}\right)^2\right], \tag{4.7}$$

and if the fetch and duration of the wind are sufficient that the dominant waves move at approximately the speed of the wind, the last factor can be replaced by $\ln(rC_\mathrm{D}^{-1})$, where C_D is the drag coefficient.

The total momentum flux to the surface layer by wave-breaking is likewise

$$\tau_w = \left(4\gamma\beta^3 I(3p+1)\frac{\rho_w}{\rho_a}\right)\rho_a g^{-\frac{1}{2}} u_*^3 (k_1^{\frac{1}{2}} - k_0^{\frac{1}{2}}), \tag{4.8}$$

which, if the range of wavenumbers in the equilibrium range is large so that $k_1 \gg k_0$, is dominated by the upper wavenumber limit to this range. Since necessarily under all conditions $\tau_w < \tau_0 = \rho_a u_*^2$, this expression in fact forces us to conclude that $k_1^{\frac{1}{2}} \propto u_*^{-1}$; with $k_1 = rg/u_*^2$, we have in a well-developed wave field that

$$\tau_w = \left[4\gamma\beta^3 I(3p+1) r^{\frac{1}{2}} \frac{\rho_w}{\rho_a}\right]\rho_a u_*^2, \tag{4.9}$$

where the coefficient in the square bracket is necessarily less than unity.

The total mean-square slope of the sea surface associated with the *gravity*-wave components can be approximated by integration of (3.8) and (3.9) over the range (k_0, k_1). In the windward direction,

$$\overline{\left(\frac{\partial\zeta}{\partial x_1}\right)_g^2} = 2\int_{-\frac{1}{2}\pi}^{\frac{1}{2}\pi}\int_{k_0}^{k_1} S_{11}(\boldsymbol{k})\, k\, \mathrm{d}k\, \mathrm{d}\theta$$

$$= 4\beta I(p+2)\, u_* g^{-\frac{1}{2}}(k_1^{\frac{1}{2}} - k_0^{\frac{1}{2}}), \tag{4.10}$$

while the total mean-square slope

$$\overline{(\nabla\zeta)^2} = 4\beta\, I(p)\, u_* g^{-\frac{1}{2}}(k_1^{\frac{1}{2}} - k_0^{\frac{1}{2}}). \tag{4.11}$$

The ratio of these clearly depends on p alone and is equal to $I(p+2)/I(p)$. Measurements of this ratio by Cox & Munk (1954), which may include contributions from capillary waves as well, range from 0.5 to 0.64, while more recent results of Tang & Shemdin (1983) in waves with a well-defined spectral peak give an average ratio of a little less than 0.5.

In a well-developed sea, with $k_1 = rg/u_*^2 \gg k_0$, the downwind mean-square slope of the gravity waves approaches

$$\overline{\left(\frac{\partial\zeta}{\partial x_1}\right)_g^2} = 4r^{\frac{1}{2}}\beta I(p+2),$$

while the crosswind contribution

$$\overline{\left(\frac{\partial\zeta}{\partial x_2}\right)^2} = 4r^{\frac{1}{2}}\beta[I(p) - I(p+2)],$$

with the total

$$\overline{(\nabla\zeta)^2} = 4r^{\frac{1}{2}}\beta I(p) = r^{\frac{1}{2}}\alpha, \tag{4.12}$$

where α is Toba's constant.

As a wind-generated wave field develops, then, the extent of the equilibrium range widens and the mean-square slope of the gravity-wave components increase towards an asymptotic value approximately equal to Toba's constant. This simple and interesting result is, however, a little hard to assess immediately in the light of observational results available at the present time. In both Cox & Munk's classical results and in Tang & Shemdin's, the contributions from the capillary waves to the mean-square slope cannot be sorted out. Nevertheless, at wind speeds greater than 10 m/s, the values of $\overline{(\nabla\zeta)^2}$ obtained by these authors for a clean sea surface and well-defined spectral peak do average to a value of about 0.06, close to the estimate of α obtained by Kawai *et al.* (1977) but less than those found by Kahma (1981) and

Forristall (1981). If the latter are more nearly correct, then $r \sim 0.3$. Perhaps the capillary-wave components do not contribute significantly to $\overline{(\nabla\zeta)^2}$ after all – if they did, the total mean-square slope would probably exceed α.

5. Constraints on the empirical constants

A number of empirical coefficients appear in this description, some of which have been measured in, or can be inferred from, different sets of experiments. However, some of the evidence is fragmentary, and troubling discrepancies do remain between different sets of measurements of the same quantity, particularly Toba's constant α. The theory given here provides certain relationships among these quantities and constraints on their magnitudes – can we use it to reduce the uncertainties that presently exist?

To summarize, the pertinent numerical coefficients and the relationships among them are as follows.

(i) p, the index in the directional distribution of $\Psi(\boldsymbol{k})$. Plant's (1982) form suggests $p = \frac{1}{2}$, while the measurements by Donelan *et al.* (1984) suggest that $p \sim 2$, though the frequencies they consider are at the very low end of the equilibrium range. The measured ratio of the mean-square slopes in the downwind direction to the total, $I(p+2)/I(p)$, averaging about 0.5, suggest, from figure 2, a *small* value of p and a wide directional distribution of the equilibrium-range components.

(ii) α, Toba's constant. Field measurements summarized in table 1 fall in the range $(6\text{–}11)\times 10^{-2}$.

(iii) β, the numerical coefficient in the wavenumber spectrum. From (3.3) and (3.4),

$$\beta = \alpha/4I(p). \tag{5.1}$$

No independent, direct and reliable measurements of β are known to the author.

(iv) r, the coefficient of order unity associated with the upper-limit wavenumber of the gravity equilibrium range.

(v) γ, the constant of proportionality in the wave-breaking dissipation function, which, according to (4.3) is such that $\gamma\beta^2$ is somewhat larger than the wind–wave coupling coefficient, approximately 0.04.

(vi) The wind-stress constraint from (4.9):

$$4\gamma\beta^3 I(3p+1)\, r^{\frac{1}{2}}\frac{\rho_w}{\rho_a} < 1,$$

or

$$\gamma\beta^3 I(3p+1)\, r^{\frac{1}{2}} < 3\times 10^{-4}. \tag{5.2}$$

Less reliably, we also have the following.

(vii) The mean-square slope asymptote $r^{\frac{1}{2}}\alpha$, possibly about 0.06.

(viii) Spectral levels of the frequency spectrum of slope in the downwind direction. Tang & Shemdin's results suggest that

$$4\beta I(p+2) \approx (3\text{–}4)\times 10^{-2}, \tag{5.3}$$

though with considerable uncertainty.

Since the quality of these data varies considerably, any attempt at optimization of the set of numerical values would be highly subjective. Let us simply consider a couple of alternatives. The mean-square slope measurements as a whole suggest a

small value of p. If $p = \frac{1}{2}$, the downwind to total mean-square slope ratio is 0.53, close to what is measured, and, if $\alpha = 11 \times 10^{-2}$, then

$$\beta = 1.2 \times 10^{-2} \quad \text{and} \quad 4\beta I(p+2) = 6.8 \times 10^{-2},$$

rather larger than the value given by (5.3). Since $\gamma\beta^2$ is somewhat larger than 0.04,

$$\gamma\beta^3 I(3p+1) > 6.7 \times 10^{-4},$$

requiring (from (5.2)) that $r^{\frac{1}{2}}$ is about 0.4 or less. This is somewhat smaller than indicated by (vii) above. If the true value of Toba's constant is less than this, say 6×10^{-2}, then $\beta = 0.7 \times 10^{-2}$ and $4\beta I(p+2) = 4 \times 10^{-2}$, which is consistent with (5.3). On the other hand, $\gamma\beta^3 I(3p+1) > 4 \times 10^{-4}$, which allows $r^{\frac{1}{2}}$ to be possibly as large as 0.7, giving $r^{\frac{1}{2}}\alpha$ rather smaller than 0.06. Consequently, a wide directional distribution of the wavenumbers in the equilibrium range in either case allows a reasonable but not perfect consistency with different sets of measurements, but requires the wind-stress inequality to be very tight – a considerable portion of the total stress in a well-developed wind-wave field must be transmitted to the water by the breaking of waves in this range.

On the other hand, a value of p of 2 would imply a downwind-to-total mean-square slope ratio of 0.75, which is considerably higher than the values measured either by Cox & Munk or Tang & Shemdin. From (5.1) if $\alpha = 11 \times 10^{-2}$, β would then be larger than before, 1.7×10^{-2}, and the inequality (5.2) is still rather tight, since $\gamma\beta^3 I(3p+1) > 6.4 \times 10^{-4}$. $4\beta I(p+2)$ is then 8×10^{-2}, rather too large when compared with (5.3). With a relatively narrow directional distribution such as $\cos^2\theta$, reasonable consistency in the measurements other than the slope ratio can be obtained only with a value of α smaller than measured by Kahma and by Forristall. It is clear that the keys to resolving these uncertainties are the accurate determination of β and the directional distribution in the equilibrium range, and it is to be hoped that remote sensing or other techniques will soon make this possible.

6. Some statistical characteristics of breaking waves

As the wind blows over the water surface, at any instant the fronts of the breaking waves define a distribution of isolated line or arc segments. The scales of the breaking waves may cover a very wide range as described earlier, from very short gravity waves in which a moving convergent stagnation point is marked by a group of capillary ripples through intermediate scales (15–30 cm or so) where the breaking is unsteady and turbulent but only a few bubbles are produced, to actual whitecaps in which the breaking and the generation of turbulence is so vigorous that extensive patches of foam are generated. There is clearly some association of the breaking events with waves of different scales, but it is difficult to make the association in an unambiguous way if we consider only the surface configuration at one given instant. A breaking crest may indeed be a local maximum in the instantaneous surface configuration but there is no guarantee that a local wavelength of the breaking wave can be defined clearly. It seems more satisfactory to use the velocity $\boldsymbol{c}$ of the breaking front as a measure of the scale of the breaking, since this is a well-defined quantity that might (conceptually at any rate) be measured from ciné images of the sea surface. In practice, it could be obtained relatively easily for those breaking events that generate whitecaps, thought it may be difficult to discern the many smaller-scale, fugitive occurrences of breaking that do not generate discernible bubble trains but which still turn over the water surface as they advance.

In any event, let us define a distribution $\Lambda(c)$ such that $\Lambda(c)\,\mathrm{d}c$ represents the average total length per unit surface area of breaking fronts that have velocities in the range c to $c+\mathrm{d}c$. The total length of breaking fronts per unit area is then

$$L = \int \Lambda(c)\,\mathrm{d}c. \tag{6.1}$$

In unit time, the fraction of sea-surface area traversed by breaking fronts with velocities between c and $c+\mathrm{d}c$ is $c\Lambda(c)\,\mathrm{d}c$, so that the fraction of total surface area turned over per unit time, the turnover rate, is

$$R = \int c\Lambda(c)\,\mathrm{d}c. \tag{6.2}$$

This quantity also expresses the total number of breaking waves of all scales passing a given point per unit time; the distribution $c\Lambda(c)\,\mathrm{d}c$ specifies the expected number per unit time passing a fixed point with velocities in the interval c to $c+\mathrm{d}c$.

What is the rate of energy loss from the waves to turbulence per unit length of front in these breaking events? This question has been examined by Duncan (1981) in a series of laboratory experiments; he showed that, in a continuing active breaker in deep water, the breaking zone extends down the forward face of the wave over a fixed fraction of its amplitude and that its shape is geometrically similar for waves of different scales. Furthermore, he found that the breaking waves themselves are geometrically similar, so that the cross-sectional area of the breaking zone is proportional to the square of the local wavelength, or to $(c^2/g)^2$. The weight of the breaking zone per unit length of the front then exerts a tangential force per unit length proportional to c^4/g that acts on the incoming stream, whose speed is approximately c. Consequently, the rate of energy loss per unit length of front is $b(c^5/g)$, where b is a numerical constant estimated by Duncan from his experiments as approximately 0.06.

It is interesting to observe, even at this stage, that the rate of turbulent-energy production increases very rapidly with the speed of advance c of the breaking front. A few large-scale breaking events can produce as much energy loss from the wave field and input to the turbulence as many smaller ones. Nevertheless, the characteristic timescale for the duration of a breaking event, the ratio of the wave energy in one wavelength to the rate of loss by breaking, is proportional to the wave period, so that, in this sense, both large- and small-scale breaking events are equally transient.

The average rate of energy loss per unit area by breakers with speeds between c and $c+\mathrm{d}c$ is then

$$\epsilon(c)\,\mathrm{d}c = bg^{-1}c^5\Lambda(c)\,\mathrm{d}c. \tag{6.3}$$

Let us now identify the scales of waves that are breaking by the speeds with which their fronts advance. For the larger-scale breaking events, i.e. those whose phase speeds $c > (2\pi s)\,C$, where C is the phase speed of the dominant wave, the associated wavenumber is simply $k = g/c^2$. The speed of advance of smaller- or microscale breaking events *is*, however, influenced strongly by long-wave advection, and this introduces a substantial complication in the transformation. One might possibly argue that breaking occurs predominantly near the crests of the dominant waves where the orbital speed is u_0, so that $k \approx g/(c-u_0\cos\theta)^2$, where θ is the angle between the breaking front and the dominant wave. This matter will not be pursued further here, however; let us concentrate on the larger-scale breaking events.

With $k = g/c^2$, an element of area $\mathrm{d}\boldsymbol{k}$ on the wavenumber plane is related to the element $\mathrm{d}\boldsymbol{c}$ on the velocity plane by

$$\begin{aligned}\mathrm{d}\boldsymbol{k} &= k\,\mathrm{d}k\,\mathrm{d}\theta,\\ &= -\frac{2g^2}{c^6}c\,\mathrm{d}c\,\mathrm{d}\theta,\\ &= -\frac{2g^2}{c^6}\mathrm{d}\boldsymbol{c},\end{aligned} \tag{6.4}$$

the negative sign being associated with the fact that integration to larger k corresponds to integration to smaller c. The rate of energy loss (4.2) in the wavenumber plane

$$\begin{aligned}\epsilon(\boldsymbol{k})\,\mathrm{d}\boldsymbol{k} &= \gamma\beta^3(\cos\theta)^{3p}\,u_*^3\,k^{-2}\,\mathrm{d}\boldsymbol{k}\\ &= \tfrac{1}{2}\epsilon(\boldsymbol{c})\,\mathrm{d}\boldsymbol{c},\end{aligned} \tag{6.5}$$

the factor $\frac{1}{2}$ arising if the direction of $\boldsymbol{c}$ is taken to lie between $-\frac{1}{2}\pi$ and $\frac{1}{2}\pi$, while that of $\boldsymbol{k}$ ranges over $-\pi$ to π. Consequently, dropping the negative sign,

$$\begin{aligned}\epsilon(\boldsymbol{c})\,\mathrm{d}\boldsymbol{c} &= 2\gamma\beta^3(\cos\theta)^{3p}\,u_*^3\,k^{-2}\,\mathrm{d}\boldsymbol{k},\\ &= 4\gamma\beta^3(\cos\theta)^{3p}\,u_*^3\,c^{-2}\,\mathrm{d}\boldsymbol{c},\end{aligned} \tag{6.6}$$

from (6.4) and (6.5), so that, from (6.3), we have for the distribution of length per unit area of breaking front per velocity element

$$\Lambda(\boldsymbol{c}) = (4\gamma\beta^3 b^{-1})\,(\cos\theta)^{3p}\,u_*^3\,gc^{-7}. \tag{6.7}$$

This distribution decreases very rapidly as c increases – those fronts associated with larger scales that produce whitecaps are evidently a very small fraction of the whole. The distribution in direction is also considerably narrower than the spectral distribution itself, which is proportional to $(\cos\theta)^p$ – a preponderance of breaking-wave events advance in directions close to that of the wind.

The expression (6.7) now enables us to estimate explicitly the expected number of breaking waves passing a given point with velocities in the interval $\boldsymbol{c}$ to $\boldsymbol{c}+\mathrm{d}\boldsymbol{c}$, $c\Lambda(\boldsymbol{c})\,\mathrm{d}\boldsymbol{c}$, or with speeds in the interval c to $c+\mathrm{d}c$ regardless of direction:

$$\begin{aligned}n(c)\,\mathrm{d}c &= \int_{-\frac{1}{2}\pi}^{\frac{1}{2}\pi} c\Lambda(\boldsymbol{c})\,c\,\mathrm{d}\theta\,\mathrm{d}c,\\ &= (4\gamma\beta^3 b^{-1} I(3p))\,u_*^3\,gc^{-5}\,\mathrm{d}c.\end{aligned} \tag{6.8}$$

The total density of breaking fronts (expected total length per unit surface area) that have speeds between c_0 and c_1 is therefore, from (6.7),

$$\begin{aligned}L(c_0,c_1) &= \int_{-\frac{1}{2}\pi}^{\frac{1}{2}\pi}\int_{c_0}^{c_1}\Lambda(\boldsymbol{c})\,c\,\mathrm{d}c\,\mathrm{d}\theta,\\ &= (\tfrac{4}{5}\gamma\beta^3 b^{-1} I(3p))\,u_*^3\,g(c_0^{-5}-c_1^{-5}),\end{aligned} \tag{6.9}$$

and the expected number passing a given point per unit time with speeds in this range is

$$\begin{aligned}n(c_0,c_1) &= \int_{c_0}^{c_1} n(c)\,\mathrm{d}c\\ &= (\gamma\beta^3 b^{-1} I(3p))\,u_*^3\,g(c_0^{-4}-c_1^{-4}).\end{aligned} \tag{6.10}$$

With the values given previously, the numerical values of the coefficients in (6.9) and (6.10) included in the brackets are both approximately 10^{-2}.

If we consider only those breaking fronts that generate a train of bubbles, the event

being then identified as a whitecap, then one might postulate that only these breaking zones with a rate of energy release bc^5/g exceeding some threshold value, ϵ_T say, will contribute. The lower limit of integration in these expressions is then $c_0 = c_T$, where

$$\epsilon_T = bc_T^5/g.$$

If, under light winds or at a short fetch, the longest waves that are breaking are shorter than those with speed c_T, then virtually no whitecaps will be formed. Yet if they are even somewhat longer, then the terms c_1^{-5} and c_1^{-4} are much smaller than c_T^{-5} and c_T^{-4} respectively. Consequently, in this case, the expected length of whitecap fronts per unit area is almost independent of the speed of the longest waves in the field, and is equal to

$$\begin{aligned} L_w &\approx (\tfrac{4}{5}\gamma\beta^3 b^{-1} I(3p))\, c_T^{-5} g u_*^3, \\ &= (\tfrac{4}{5}\gamma\beta^3 I(3p))\, \epsilon_T^{-1} u_*^3, \end{aligned} \tag{6.11}$$

while the expected number passing a given point per unit time

$$n_w = (\gamma\beta^3 b^{-1} I(3p))\, c_T^{-4} g u_*^3, \tag{6.12}$$

both increasing as the cube of the friction velocity.

There are, unfortunately, no measurements yet available with which these expressions can be compared in a significant way. They are certainly related, though somewhat tenuously, to that rather ill-defined oceanographic statistic, the degree of whitecap coverage, or the fraction of surface area covered by bubbles. If bubbles, once generated, persist for an average time T on the surface, then the whitecap coverage is

$$W = \int cT\Lambda(\boldsymbol{c})\, \mathrm{d}\boldsymbol{c}.$$

Now T is likely to depend on the surface temperature, atmospheric humidity and various surface properties not well understood; if we simply suppose it to be a constant, then by a similar calculation,

$$W \approx (\gamma\beta^3 b^{-1} I(3p))\, T c_T^{-4} g u_*^3, \tag{6.13}$$

where c_T is the slowest speed of fronts capable of producing whitecaps, provided, of course, the fastest breaking waves are moving more rapidly than this. Although the accuracy of this estimate is likely to be low (matching, indeed the considerable scatter in reported measurements of the whitecap coverage), the wind-speed dependence that it exhibits is close to, but a little less than, those found empirically. Fitting observations to the form $W \propto U^n$, Monahan (1971) found $n \sim 3.4$, Tang (1974) gives $n = 3.2$, Wu (1979) 3.75 and Monahan & Muircheartaigh (1980) 3.52 or 3.41.

It is a pleasure to acknowledge many useful discussions with colleagues and friends, particularly S. A. Kitaigorodskii, Y. Toba and H. Mitsuyasu, and also the support of the Fluid Dynamics Branch of the Office of Naval Research under contract N00014-76-C-0184.

REFERENCES

Banner, M. L. & Melville, W. K. 1976 On the separation of air flow over water waves. *J. Fluid Mech.* **77**, 825–842.

Beal, R. C., DeLeonibus, P. S. & Katz, I. 1981 *Spaceborne Synthetic Aperture Radar for Oceanography*. The Johns Hopkins Press.

Cox, C. S. 1958 Measurements of slopes of high-frequency wind waves. *J. Mar. Res.* **16**, 199–225.

DONELAN, M. A., HAMILTON, J. & HUI, W. H. 1984 Directional spectra of wind-generated waves. *Phil. Trans. R. Soc. Lond.* A (in press).

DUNCAN, J. H. 1981 An experimental investigation of breaking waves produced by a towed hydrofoil. *Proc. R. Soc. Lond.* A **377**, 331–348.

FORRISTALL, G. Z. 1981 Measurements of a saturated range in ocean wave spectra. *J. Geophys. Res.* **86**, 8075–8084.

FOX, M. J. H. 1976 On the nonlinear transfer of energy in the peak of a gravity-wave spectrum. II. *Proc. R. Soc. Lond.* A **348**, 467–483.

GENT, P. R. & TAYLOR, P. A. 1976 A numerical model of the air flow above water waves. *J. Fluid Mech.* **77**, 105–128.

HASSELMANN, K. 1962 On the non-linear energy transfer in a gravity wave spectrum. Part 1. *J. Fluid Mech.* **12**, 481–500.

HASSELMANN, K. 1963 On the non-linear energy transfer in a gravity wave spectrum. Parts 2 and 3. *J. Fluid Mech.* **15**, 273–281; 385–398.

HASSELMANN, K. *et al.* 1973 Measurements of wind wave growth and swell decay during the Joint North Sea Wave Project (JONSWAP). *Herausgegeben vom Deutsch–Hydrograph. Inst., Reihe* A, no. 12.

KAHMA, K. K. 1981 A study of the growth of the wave spectrum with fetch. *J. Phys. Oceanogr.* **11**, 1503–1515.

KAWAI, S., OKUDA, K. & TOBA, Y. 1977 Field data support of three-seconds power law and $gu_*\sigma^{-4}$ spectral form for growing wind waves. *J. Oceanogr. Soc. Japan* **33**, 137–50.

KEULEGAN, J. H. 1951 Wind tides in small closed channels. *J. Res. Natl Bur. Stand.* **46**, 358–381.

KITAIGORODSKII, S. A. 1983 On the theory of the equilibrium range in the spectrum of wind-generated gravity waves. *J. Phys. Oceanogr.* **13**, 816–827.

KITAIGORODSKI, S. A. 1984 On the fluid dynamical theory of turbulent gas transfer across an air–sea interface in the presence of breaking waves. *J. Phys. Oceanogr.* **14**, 960–972.

KOMEN, G. J., HASSELMANN, S. & HASSELMANN, K. 1984 On the existence of a fully developed wind-sea spectrum. *J. Phys. Oceanogr.* **14**, 1271–1285.

LONGUET-HIGGINS, M. S. 1976 On the nonlinear transfer of energy in the peak of a gravity-wave spectrum: a simplified model. *Proc. Roy. Soc. Lond.* A **347**, 311–328.

LONGUET-HIGGINS, M. S., CARTWRIGHT, D. E. & SMITH, N. D. 1963 Observations of the directional spectra of sea waves using the motion of a floating buoy. In *Ocean Wave Spectra*, pp. 111–136. Prentice-Hall.

LONGUET-HIGGINS, M. S. & COKELET, E. D. 1978 Growth of normal mode instabilities. *Proc. R. Soc. Lond.* A **364**, 1–28.

MILES, J. W. 1957 On the generation of surface waves by shear flow. *J. Fluid Mech.* **3**, 185–204.

MITSUYASU, H. *et al.* 1975 Observations of the directional spectra of ocean waves using a cloverleaf buoy. *J. Phys. Oceanogr.* **5**, 750–760.

MITSUYASU, H. *et al.* 1980 Observation of the power spectrum of ocean waves using a cloverleaf buoy. *J. Phys. Oceanogr.* **10**, 286–296.

MITSUYASU, H. & HONDA, T. 1982 Wind-induced growth of water waves. *J. Fluid Mech.* **123**, 425–442.

MONAHAN, E. C. 1971 Oceanic whitecaps. *J. Phys. Oceanogr.* **1**, 139–144.

MONAHAN, E. C. & MUIRCHEARTAIGH, I. 1980 Optimal power-law description of oceanic whitecap coverage dependence on wind speed. *J. Phys. Oceanogr.* **10**, 2094–2099.

PHILLIPS, O. M. 1958 The equilibrium range in the spectrum of wind-generated ocean waves. *J. Fluid Mech.* **4**, 426–434.

PHILLIPS, O. M. 1977 *The Dynamics of the Upper Ocean.* Cambridge University Press.

PHILLIPS, O. M. 1981 The dispersion of short wavelets in the presence of a dominant long wave. *J. Fluid Mech.* **107**, 465–485.

PHILLIPS, O. M. 1984 On the response of short ocean wave components at a fixed wave number to ocean current variations. *J. Phys. Oceanogr.* **14**, 1425–1433.

PHILLIPS, O. M. & BANNER, M. L. 1974 Wave breaking in the presence of wind drift and swell. *J. Fluid Mech.* **66**, 625–640.

PIERSON, W. J. (ed.) 1962 The directional spectrum of a wind-generated sea as determined from data obtained by the Stereo Wave Observation Project. *Coll. Engng NYU Met. Pap.* **2**, no. 6.

PLANT, W. J. 1982 A relationship between wind stress and wave slope. *J. Geophys. Res.* **87**, 1961–1967.

RAMAMONJIARISOA, A. & COANTIC, M. 1976 Loi expérimental de dispersion des vagues produites par le vent sur une faible longueur d'action. *C. R. Acad. Sci. Paris* B **282**, 111–113.

SCHULE, J. J., SIMPSON, L. S. & DELEONIBUS, P. S. 1971 A study of fetch limited wave spectra with an airborne laser. *J. Geophys. Res.* **76**, 4160–4171.

SELL, W. & HASSELMANN, K. 1972 Computation of nonlinear energy transfer for JONSWAP and empirical wind wave spectra. *Rep. Inst. Geophys., Univ. Hamburg.*

SNYDER, R. L., DOBSON, F. W., ELLIOTT, J. A. & LONG, R. B. 1981 Array measurements of atmospheric pressure fluctuations above surface gravity waves. *J. Fluid Mech.* **102**, 1–59.

TANG, C. C. H. 1974 The effect of droplets in the air–sea transition zone on the mean brightness temperature. *J. Phys. Oceanogr.* **4**, 579–593.

TANG, S. & SHEMDIN, O. H. 1983 Measurements of high frequency waves using a wave follower. *J. Geophys. Res.* **88**, 9832–9840.

TOBA, Y. 1973 Local balance in the air–sea boundary processes. III. On the spectrum of wind waves. *J. Oceanogr. Soc. Japan* **29**, 209–220.

WU, J. 1979 Oceanic whitecaps and sea state. *J. Phys. Oceanogr.* **9**, 1064–1068.